Journal of Energy Storage 75 (2024) 109735

Contents lists available at ScienceDirect

Journal of Energy Storage

journal homepage: www.elsevier.com/locate/est

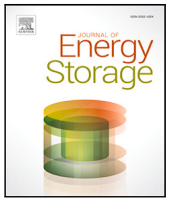

Research papers

Packed bed thermal energy storage for waste heat recovery in the iron and steel industry: A cold model study on powder hold-up and pressure drop

Paul Schwarzmayr [a,*], Felix Birkelbach [a], Heimo Walter [a], Florian Javernik [b], Michael Schwaiger [b], René Hofmann [a]

[a] Institute for Energy Systems and Thermodynamics, TU Wien, Getreidemarkt 9, Vienna, 1060, Austria
[b] voestalpine Stahl Donawitz GmbH, Kerpelystraße 199, Leoben, 8700, Austria

ARTICLE INFO

Keywords:
Packed bed thermal energy storage
Gas-powder two phase flow
Powder hold-up
Pressure drop
Exergy efficiency
Iron/steel industry

ABSTRACT

Waste heat recovery in the energy intensive industry is one of the most important measures for the mitigation of climate change. The present study examines the integration of a packed bed thermal energy storage for waste heat recovery in the iron and steel industry. Along with the highly fluctuating availability of excess heat the main difficulty of waste heat recovery in industrial processes is the high amount of powder that is transported by the hot exhaust gases. Therefore, the experimental investigations in this study focus on the powder hold-up and pressure drop in a packed bed thermal energy storage that is operated with a gas-powder two phase exhaust gas as heat transfer fluid. The ultimate goal is, to assess its suitability and robustness under such challenging operational conditions. The results indicate, that 98 % of the powder that is introduced into the system with the heat transfer fluid during charging accumulates in the packed bed. Remarkably, most of the powder hold-up in the packed bed is concentrated near the surface at which the heat transfer fluid enters the packed bed. When reversing the flow direction of the heat transfer fluid to discharge the storage with a clean single phase gas, this gas is not contaminated with the powder that has been accumulated in previous charging periods. The entirety of these findings reinforces the suitability of packed bed thermal energy storage systems for waste heat recovery in the energy intensive industry.

1. Introduction

The waste heat potential from the industry sector is enormous and its exploitation can lead to substantial primary energy savings. The biggest challenge of waste heat recovery is, that the utilization of only a fraction of the theoretical waste heat potential (approx. one third in 2014) is economically feasible. This is mainly because of techno-economic constraints like minimum temperature requirements, discontinuous waste heat availability, technology costs, or even the lack of suitable technologies. A comprehensive review considering the implementation of thermal energy storage (TES) systems for industrial waste heat recovery is provided by Miró et al. [1]. In a similar study Manente et al. [2] stated, that one of the most suitable types of TES for industrial waste heat recovery is a packed bed thermal energy storage (PBTES). Since PBTES systems use a non-pressurized steel vessel as storage tank, rocks or some other type of solids as storage material and a gaseous medium as heat transfer fluid (HTF) they are extremely cost efficient and require little maintenance.

Contrary to the maturity of PBTES systems for their integration into concentrated solar power (CSP) plants [3,4] studies on their utilization as industrial waste heat recovery systems are rare. The biggest difference between integrating a PBTES into an industrial waste heat recovery system and into a CSP plant is the composition of the HTF. In a CSP plant a PBTES system is charged and discharged with clean air whereas in an industrial waste heat recovery system the HTF will be some kind of gas-powder two phase exhaust gas. In their studies on the utilization of a PBTES for waste heat recovery in industrial processes Ortega-Fernández et al. [5] and Slimani et al. [6] dealt with this issue by placing a high temperature dust filter and a gas-to-gas heat exchanger between the industrial waste heat source and the TES so that the TES can be operated with clean air. However, this approach is far from optimal, because the filtration of high temperature gas is difficult and expensive and the exergy efficiency of gas-to-gas heat exchangers is low. Additionally the lifetime of these heat exchangers would be short due to the abrasiveness of the gas-powder two phase exhaust gas. Therefore, the authors of the present study consider the

* Corresponding author.
E-mail addresses: paul.schwarzmayr@tuwien.ac.at (P. Schwarzmayr), michael.schwaiger@voestalpine.com (M. Schwaiger), rene.hofmann@tuwien.ac.at (R. Hofmann).

https://doi.org/10.1016/j.est.2023.109735
Received 31 July 2023; Received in revised form 23 October 2023; Accepted 12 November 2023
Available online 16 November 2023

Nomenclature

Acronyms

CSP	Concentrated solar power
HTF	Heat transfer fluid
LD	Linz–Donawitz
PBTES	Packed bed thermal energy storage
TES	Thermal energy storage

Roman symbols

$\overline{d}$	Sauter diameter in m
Eu	*Euler*-number
L	Packed bed height in m
Δp	Pressure drop in Pa
$\Delta\hat{p}$	Relative pressure drop
p	Pressure in Pa
r_0	Characteristic length of a non-spherical packed bed particle in m
Re	*Reynolds*-number
v	Superficial fluid velocity in $\mathrm{m\,s^{-1}}$

Greek symbols

δ_0	Characteristic length for the fluid flow path in m
η	Dynamic viscosity of the fluid in Pa s
Φ_D	Shape factor for non-spherical packed bed particles
ψ	Fractional void volume in $\mathrm{m^3\,m^{-3}}$
ρ	Mass density of the fluid in $\mathrm{kg\,m^{-3}}$

Subscripts

f	Fluid
i	Index of pressure measuring point
j	Index of pressure measuring point
n	Sample number
p	(packed bed) Particle

direct use of high temperature gas-powder two phase exhaust gas from industrial processes as HTF for charging a PBTES. A schematic view of the proposed waste heat recovery system is depicted in Fig. 1. This approach drastically decreases investment (no high temperature filtration, no additional heat exchanger) and maintenance costs (filter, heat exchanger) of the whole system. In order to make assessments on the suitability and robustness of a PBTES system in such a setting this study examines the behavior of a PBTES system that is operated with a gas-powder two phase exhaust gas as HTF.

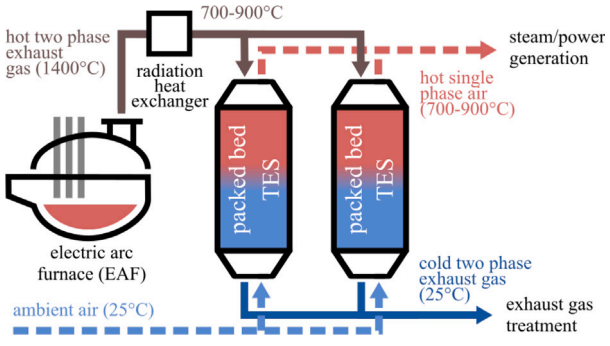

Fig. 1. Integration of PBTES systems for the waste heat recovery from industrial exhaust gas.

The first studies that consider gas-powder two phase flows in packed beds date back to the early 1990s and were conducted to investigate the behavior of coal powder that is injected into a blast furnace. In the most recent study from Gupta et al. [7] the authors state that despite the variety of publications considering this topic [8–12], the literature reveals that consistency is lacking and that the behavior of gas-powder two phase flow in packed beds is still not fully understood yet. Additionally, the application of experimental results that were generated in the context of pulverized coal injection into a blast furnace to a PBTES that is operated with a gas-powder two phase HTF is impracticable. Operational conditions that prevail in a blast furnace are fundamentally different to the conditions in a PBTES. Probably the biggest difference is, that in a blast furnace the powder (pulverized coal) undergoes a chemical reaction either with the gaseous part of the flowing fluid (burning) or the packed bed particles (reduction of iron ore) whereas in a PBTES the interactions between the packed bed and the HTF are limited to heat transfer, momentum transfer and adhesion. In a blast furnace coal powder with a narrow particle size distribution and a median particle size of 75 µm is laterally injected into the bottom of the packed bed. In a PBTES that is operated with a gas-powder two phase HTF the gas-powder flow enters the packed bed through the top surface. Furthermore, the particle size distribution of metal dust from a steel producing processes is much wider with a median particle size of less than 10 µm. Therefore, the authors of this study decide to build upon existing research on gas-powder two phase flows in packed beds that was conducted in the context of coal powder injection into blast furnaces and to apply and extend this area of research towards PBTES systems that are operated with a gas-powder two phase HTF.

The remainder of this paper includes a presentation of the test rig that is designed and erected for the experimental investigations in Section 2. Additionally, properties and other information about the materials that are used for the packed bed and the powder are summarized in Section 2. Section 3 delineates the data analysis procedure and empirical pressure drop equations that are used for measurement data validation. Section 4 includes the presentation of all the results from the experiments as well as an interpretation of these results with the ultimate goal to assess the suitability of PBTES systems for waste heat recovery in the iron and steel industry.

2. Material and methods

2.1. Experimental setup

To investigate the powder hold-up and pressure drop in a PBTES when it is operated with a gas-powder two phase HTF, a lab-scale cold model test rig of a vertical PBTES is used. Fig. 2 shows a P&ID of the cold model test rig with all its components and instrumentation. The storage tank itself is a vertical acrylic glass cylinder with a height to diameter ratio of approximately 3 and is filled with 68.5 kg of storage material. The storage material and the powder for the experiments were chosen in a way, that the operational conditions are comparable with an industrial scale PBTES. As storage material slag, a by-product from the iron and steel industry, is used. In addition to the extremely low costs, the suitability of slag as storage material for a PBTES is justified by its good heat transfer properties due to its geometric shape. The irregular shaped and partly porous rocks that the slag is composed of lead to a uniform random packing, hence an even perfusion, and a high volume-specific surface of the packed bed, hence an improved heat transfer between HTF and storage material. More details about the storage tank's geometry and properties of the storage material are summarized in Table 1. For the experiments the storage tank is equipped with 11 pressure measuring points (PT1, PT2, . . . , PT11) that are evenly distributed over the height of the packed bed. Piezoresistive pressure sensors are used to record the pressure differences between each of the pressure measuring points in the storage tank. Before the experiments the piezoresistive sensors are calibrated to an accuracy of

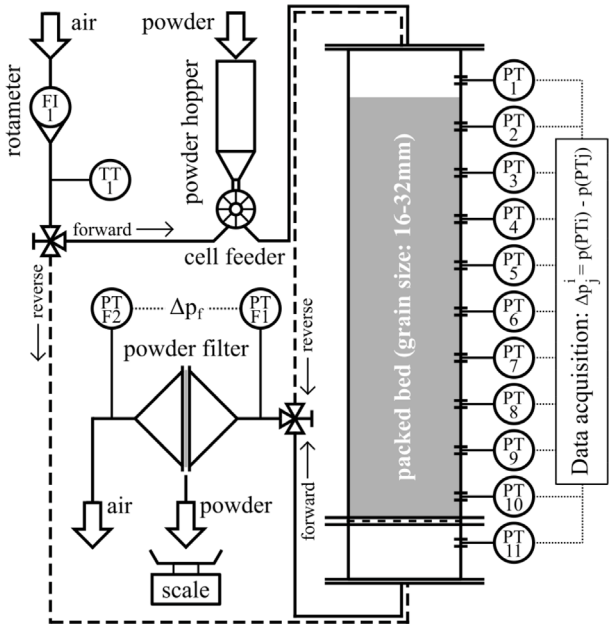

Fig. 2. Experimental test rig.

±0.06% of full scale. The flow rate of the HTF (dry, clean and cold ambient air provided by an air supply unit) into the system is controlled with a rotameter flow meter.

To simulate a charging process of the PBTES cold model with a gas-powder two phase flow the initially clean HTF (cold ambient air) is directed to a cell feeder where powder is added before it enters the PBTES storage tank. The feed rate of the powder can be controlled by adjusting the rotational speed of the cell feeder. In order to represent reality as accurately as possible metal dust collected from the exhaust gases of a steel producing process is utilized as powder for the experiments. In Fig. 3, the particle size distribution of the powder is provided. These data are measured with a laser diffraction particle size analyzer (Malvern® Mastersizer 2000 [13]) that is fed with a dry sample dispersion unit (Malvern® Aero S [14]). The particle size distribution of the powder depicted in Fig. 3 is the average of 12 consecutive measurements. The particle size of this type of powder ranges from 0.2 µm to 600 µm with a median of 8.85 µm where the most common sizes are 3.5 µm and 350 µm. Detailed information about the metal dust are provided in Table 1. Downstream of the cell feeder the gas-powder two phase HTF enters the storage tank from the top, passes through the packed bed and leaves the tank at the bottom. Before the HTF exits the system it passes through a powder filter that separates the remaining powder from the HTF flow. The path of the HTF flow for a charging process is indicated with solid lines in Fig. 2.

For the simulation of a discharging process of the PBTES cold model with clean single-phase HTF, air from the rotameter directly enters the storage tank from the bottom, passes through the packed bed and leaves the tank at the top. Again, the air that exits the storage tank is directed through the powder filter before it is released into the environment. The HTF flow path for the discharging process is indicated with dashed lines in Fig. 2.

2.2. Experimental procedure

Before the actual experiments with gas-powder two phase flow, the pressure drop curve of clean HTF passing through the clean packed bed depending on the HTF mass flux is recorded. For these experiments the HTF mass flux is set between 0 kg m^{-2} s^{-1} to 0.6 kg m^{-2} s^{-1}. The upper limit was chosen because a further increase of the HTF mass flux would increase the pressure drop and the thickness of the thermocline which both mean a low exergy efficiency of the PBTES. Empirical equations from the literature are utilized to reconstruct and validate the measured data.

Table 1
Summary of parameters: Test rig geometry, data/properties of storage material, HTF and powder.

Test rig	
Storage type	vertical PBTES
Diameter of pipes	46 mm
Tank diameter	238 mm
Tank height	780 mm
Tank volume	0.034 m^3
Packed bed height	700 mm
Packed bed volume	0.031 m^3
Packed bed mass	68.5 kg
Packed bed material	
Type of material	slag (irregular shaped, partly porous)
Particle size	16 mm to 32 mm
Sauter-diameter $\overline{d}_p$	19.4 mm (calculation see [15])
Particle density	3800 kg m^{-3}
Void fraction	0.42
Bulk density	2200 kg m^{-3}
Shape factor (Φ_D)	0.8 [15]
volume-specific heat transfer coefficient	$\approx 11 \times 10^3$ W m^{-3} K^{-1}
Reynolds-number Re = $\rho_f\, v\, \overline{d}_p/(\psi\, \eta)$	750 to 1000
Euler-number (see Equation (3))	6.8 to 7.3
Heat transfer fluid	
Type of fluid	Air (T = 294.15 K)
Density	1.205 kg m^{-3}
Dynamic viscosity	18.23×10^{-6} Pa s
HTF mass flux	0.3 and 0.4 kg m^{-2} s^{-1}
Powder content	0.025 kg to 0.045 kg powder per kg air
Powder	
Type of material	metal dust from the iron and steel industry
Particle size	0.2 µm to 600 µm
Composition	≈95% Iron(III) oxide (Fe_2O_3) +5% of other transition metal oxides
Powder mass flux	7.5 g m^{-2} s^{-1} to 13.5 g m^{-2} s^{-1} and 10 g m^{-2} s^{-1} to 18 g m^{-2} s^{-1}

For the core experiments of this study, the cell feeder is used to produce a gas-powder two phase flow with a relative powder content of 25 g to 45 g powder per kg air which is representative for the powder content of exhaust gas from state-of-the-art steel producing processes (LD-converter and electric arc furnace). This gas-powder two phase flow further passes through the whole system as described in Section 2.1. The increase in pressure drop in the packed bed is measured with the differential pressure sensors PT1, PT2, …, PT11. The amount of powder hold-up inside the packed bed is determined via a mass

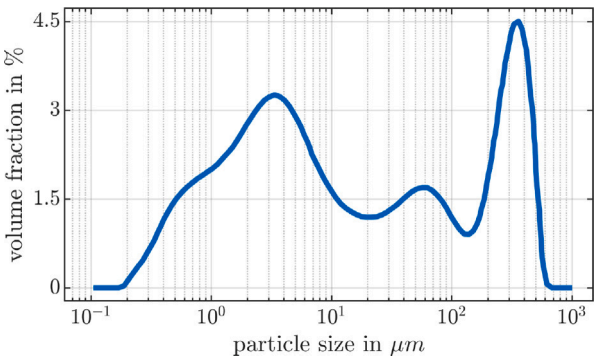

Fig. 3. Particle size distribution of the powder used for the experiments.

balance by measuring the amount of powder that is feed into the HTF flow from the powder hopper and the amount of powder that is separated from the HTF in the powder filter after passing through the packed bed. This mass balance is evaluated periodically by removing the powder filter from its housing to record its mass increase. At each time, the powder filter is cleaned before it is put back into its housing to prevent the exponentially rising pressure drop of the powder filter to impact the behavior of the remaining system. For this purpose, the test rig is equipped with two parallel powder filters so that one filter can be removed and weighed without having to interrupt the experiments. When the pressure drop of the packed bed reaches a certain threshold the charging process with gas powder two phase flow is stopped. For the experiments in this study the pressure threshold is set to 1000 Pa since this is the maximum pressure difference that can be recorded by the measurement equipment. After stopping the charging process, the flow direction of the HTF is reversed to simulate a discharging process of the PBTES with clean HTF. Clean air passes through the packed bed from the bottom to the top and exits the system through the powder filter. The reduction in pressure drop and powder hold-up is measured and determined as before. This whole procedure is repeated for a HTF mass flux of 0.3 and 0.4 $\mathrm{kg\,m^{-2}\,s^{-1}}$.

The results of these experiments can be transferred and applied to larger devices if certain similarity criteria (*Reynolds*- and *Euler*-number) are satisfied. Values for the *Reynolds*- and *Euler*-number are given in this section and in Table 1.

3. Theory and calculations

For the validation of the measured data empirical equations from the literature are used. According to Kast et al. [15] there are two different ways to model the pressure drop in a fluid passing through a packed bed. The first and simpler option is, to model the packed bed as several pipes connected in parallel which leads to the *Ergun*-equation [16]. With this equation the pressure drop per unit length can be calculated as

$$\frac{\Delta p}{\Delta L} = 150\,\frac{(1-\psi)^2}{\psi^3}\,\frac{\eta\,v}{\overline{d}_\mathrm{p}^2} + 1.75\,\frac{1-\psi}{\psi^3}\,\frac{\rho_\mathrm{f}\,v^2}{\overline{d}_\mathrm{p}} \tag{1}$$

where ψ is the fractional void volume in the packed bed, $\overline{d}_\mathrm{p}$ is the Sauter-diameter of the packed bed material, η is the dynamic viscosity of the fluid, v is the superficial fluid velocity and ρ_f is the mass density of the fluid. At this point it should be mentioned, that *Ergun*'s-equation is included in this study because it is the most common equation used to calculate the pressure drop in packed beds in the literature. However, one main disadvantage of the modeling approach used by *Ergun* is that the real flow paths of the fluid are only insufficiently considered. Detailed information on the limitations of *Ergun*'s-equation are provided by Kast et al. [15].

A more versatile but also more complex equation for the calculation of the pressure drop per unit length is the *Molerus*-equation. This equation was deduced based on the fluid flow around single packed bed particles and therefore allows a much more detailed modeling of the fluid flow paths within a packed bed with uniform randomly packed particles. By postulating equilibrium between the resistance force exerted by the fluid to each packed bed particle and the force due to the pressure drop in the fluid, Molerus [17] found that

$$\frac{\Delta p}{\Delta L} = \frac{3}{4}\,\frac{\rho_\mathrm{f}\,v^2}{\overline{d}_\mathrm{p}}\,\frac{1-\psi}{\psi^2}\,\mathrm{Eu}\left(\Phi_\mathrm{D}\right) \tag{2}$$

where

$$\mathrm{Eu}\left(\Phi_\mathrm{D}\right) = \frac{24}{\mathrm{Re}\,\Phi_\mathrm{D}^2}\left\{1 + 0.685\left[\frac{r_0}{\delta_0} + 0.5\left(\frac{r_0}{\delta_0}\right)^2\right]\right\} + \frac{4}{\sqrt{\mathrm{Re}}\,\Phi_\mathrm{D}^{1.5}}\left[1 + 0.289\left(\frac{r_0}{\delta_0}\right)^{1.5}\right] + \frac{1}{\Phi_\mathrm{D}}\left[0.4 + 0.514\,\frac{r_0}{\delta_0}\right]. \tag{3}$$

The *Euler*-number $\mathrm{Eu}\left(\Phi_\mathrm{D}\right)$ in Eq. (3) is a function of the packed bed particle *Reynolds*-number Re, a factor Φ_D that accounts for the non-spherical shape of the packed bed particles and a length ratio r_0/δ_0 which is characteristic for the geometry of the fluid flow path between the packed bed particles. For a packed bed with a fractional void volume ψ and uniform randomly packed particles the *Reynolds*-number Re and the length ratio r_0/δ_0 can be calculated as

$$\mathrm{Re} = \frac{\rho_\mathrm{f}\,v\,\overline{d}_\mathrm{p}}{\psi\,\eta} \quad \text{and} \quad \frac{r_0}{\delta_0} = \left[\frac{0.95}{\sqrt[3]{1-\psi}} - 1\right]^{-1}. \tag{4}$$

3.1. Data processing and uncertainty analysis

For a compact presentation of the most important findings of the present study the measured data from the experiments is processed using Eq. (5). In this equation the pressure measurements from any two pressure measuring points p_i and p_j are used to compute the relative pressure drop between to measuring point $\Delta\hat{p}_{\mathrm{i-j}}(n)$.

$$\Delta\hat{p}_{\mathrm{i-j}}(n) = \frac{\Delta p_{\mathrm{i-j}}(n)}{\Delta p_{\mathrm{i-j}}(n=1)} = \frac{p_i(n) - p_j(n)}{p_i(n=1) - p_j(n=1)} \tag{5}$$

The relative pressure drop between two measuring points $\Delta\hat{p}_{\mathrm{i-j}}(n)$ is the ratio of the pressure difference of the n^{th} sample $\Delta p_{\mathrm{i-j}}(n)$ and the pressure difference of the first sample, i.e. the clean bed, $\Delta p_{\mathrm{i-j}}(n=1)$.

To estimate the impact of uncertainties of the measurement devices on the results presented in this study an uncertainty analysis using the law of error propagation is conducted. As mentioned in Section 2.1, piezoresistive sensors with an accuracy of ±0.06 % of full scale are used to measure pressure differences between the measuring points in the test rig's packed bed. With a full scale of 2000 Pa (measurement range of ±1000 Pa) the utilized sensors deliver measurements with an accuracy of ±1.2 Pa. As the calculation of $\Delta\hat{p}_{\mathrm{i-j}}(n)$ in Eq. (6) requires two differential pressure measurements ($\Delta p_{\mathrm{i-j}}(n)$ and $\Delta p_{\mathrm{i-j}}(n=1)$), the law of error propagation is used to calculate the uncertainty of the relative pressure drop as

$$\delta\Delta\hat{p}_{\mathrm{i-j}}(n)^2 = \left(\frac{\delta\Delta p_{\mathrm{i-j}}(n)}{\Delta p_{\mathrm{i-j}}(n=1)}\right)^2 + \left(-\frac{\Delta p_{\mathrm{i-j}}(n)\,\delta\Delta p_{\mathrm{i-j}}(n=1)}{\Delta p_{\mathrm{i-j}}(n=1)^2}\right)^2. \tag{6}$$

The relative uncertainty of $\Delta\hat{p}_{1-11}(n)$ and $\Delta\hat{p}_{1-3}(n)$ with respect to the calculated value are well below ±2% and ±8.5% respectively. These uncertainties are insignificant compared to the scattering of the experimental data (see Figs. 6, 9 and 10) and therefore do not have an impact on the quality of the results presented in Section 4.

4. Results and discussion

To guarantee consistency and reproducibility of the measured data, the pressure drop curve of the clean packed bed is recorded three times before the core experiments. Between each of these three measurements the test rig's tank is emptied and refilled again. The results of these experiments are plotted in Fig. 4 as blue circles. It can be seen, that the data is only slightly scattered in vertical direction which indicates reproducibility of the results. Furthermore, empirical equations from *Ergun* and *Molerus* are used to compare the measured data. The parameters used for the *Ergun*- and *Molerus*- equation are documented in Table 1 which are either obtained from data sheets or from the literature [15]. Both equations (dashed lines) fit the experimental data (blue circles and solid blue line) very well as it can be seen in Fig. 4. Thereby it can be confirmed that the test rig used for the experiments in the present study delivers results that are consistent and follow the trend as predicted by the *Ergun* and *Molerus* equations.

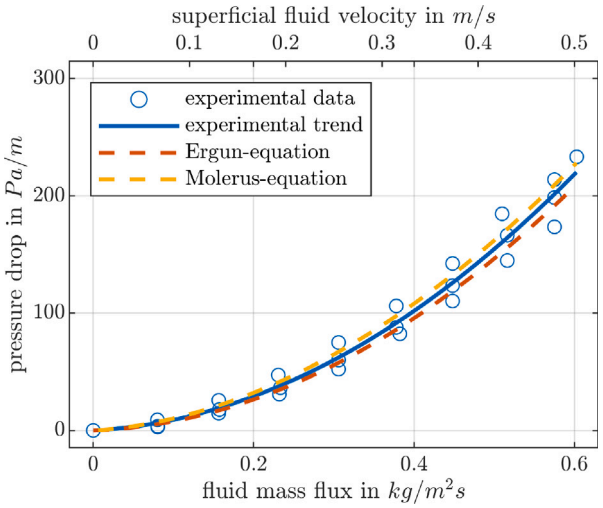

Fig. 4. Pressure drop curve of clean HTF passing through a clean and dusty packed bed.

4.1. Powder hold-up

The amount of powder that accumulates in the packed bed during a charging process (powder hold-up) is determined by measuring the amount of powder that is fed into the system by the cell feeder and the amount of powder that accumulates in the powder filter. The experiments reveal, that for a fluid mass flux of $0.4\,\mathrm{kg\,m^{-2}\,s^{-1}}$ approximately 98 % of the powder accumulates in the packed bed during a charging process. This means, that the PBTES does not only act as a thermal storage, but also as a dust collector. For an industrial scale PBTES that is operated at high temperatures this means that the HTF that exits the PBTES during a charging process is not only cold but also carries just 2 % of the amount of powder than the HTF that enters the PBTES. Furthermore, discharging the storage with clean air that passes through the contaminated packed bed in the opposite direction does not lead to a reduction of the powder hold-up in the packed bed. This is confirmed by evaluating the powder mass balance during all the discharging phases. Hence, clean air that is used to discharge the PBTES is not contaminated with powder that has been accumulated in the packed bed in a previous charging process.

One of the most interesting observations from the experiments is the axial distribution of pressure drop and powder hold-up in the packed bed which is visualized in Fig. 5. In this plot the left ordinate represents the normalized height of the packed bed and the right ordinate shows the positions of the pressure sensors. On the abscissa, the pressure drop between measuring point i and the bottom of the packed bed relative to the total pressure drop of the clean packed bed is given. The blue solid line with ∘-markers represents the relative pressure drop curve for the clean packed bed. The rest of the lines show the relative pressure drop curve of the packed bed after it was charged with gas-powder two phase flow for different periods of time. While the initial pressure drop curve (0 min) and the pressure drop curve recorded after 20 min of gas-powder two phase flow are linear functions of the packed bed height, the other two curves show different results that suggest a nonuniform distribution of powder hold-up in vertical direction. After 60 min of charging with gas-powder two phase flow (yellow dotted line) one half of the total pressure drop is caused only by the top layer (0.08 m, 11 % of the packed bed's total height) of the packed bed. These observations indicate that most of the powder that accumulates in the packed bed is concentrated at the surface where the two phase HTF enters the packed bed. Similar results are presented in Fig. 6.

This plot shows the relative pressure drop of the upper fifth of the packed bed – where the gas-powder two phase flow enters the packed bed – on the left ordinate ($\Delta\hat{p}_{1-3}$) and the relative pressure drop of the remaining height of the packed bed on the right ordinate ($\Delta\hat{p}_{3-11}$). The amount of powder hold-up in the packed bed is plotted on the abscissa. Both graphs start at a powder hold-up of $0\,\mathrm{kg\,m^{-2}}$ (clean bed) and increase with the powder hold-up in the packed bed. It can clearly be seen that the pressure drop in the upper fifth of the bed rises exponentially whereas the pressure drop in the lower region of the packed bed seems to flatten. At a powder hold-up of $40\,\mathrm{kg\,m^{-2}}$ the pressure drop in the upper fifth already increased by a factor of 8 while the pressure drop in the lower region of the packed bed has not even doubled. These results too suggest, that a large part of the powder that is introduced into a PBTES accumulates near the surface at which the gas-powder two phase flow enter the packed bed. The small portion of the powder that is further transported into the system is distributed inside the packed bed considerably uniform. These results are supported by the data presented in Fig. 7.

The left ordinate and the blue bars in this figure represent the pressure drop between two measuring points i and j. The abscissa indicates the indices of measuring points between which the presented data is measured. On the right ordinate the void fraction of the packed bed is

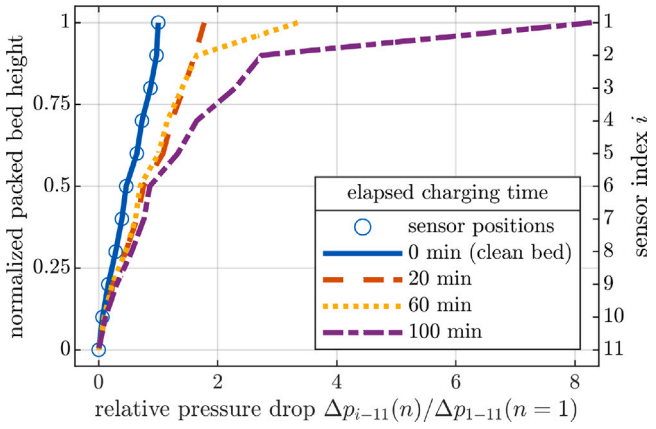

Fig. 5. Vertical/axial distribution of the pressure drop in a packed bed with powder hold-up.

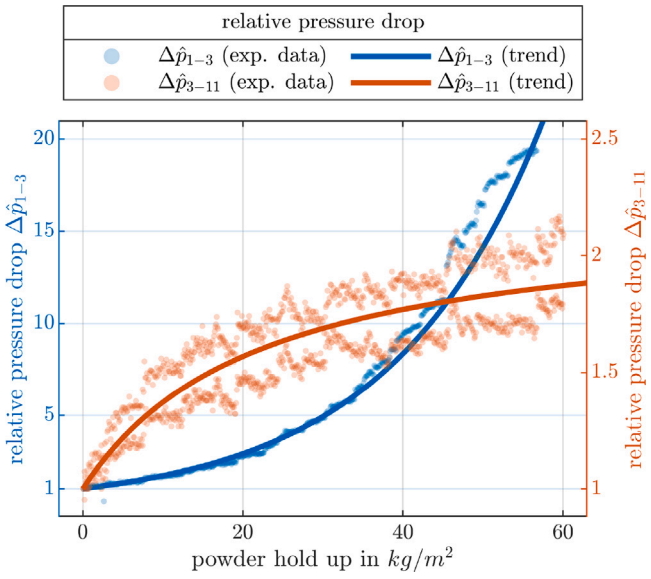

Fig. 6. Pressure drop in a packed bed with powder hold-up at different vertical/axial positions.

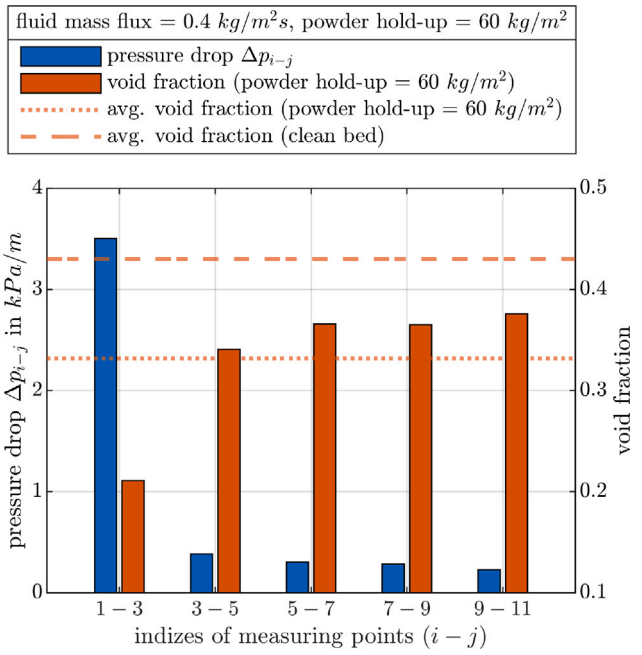

Fig. 7. Pressure drop and void fraction of a PBTES with a fluid mass flux of $0.4\,\mathrm{kg\,m^{-2}\,s^{-1}}$ and a powder hold-up of $60\,\mathrm{kg\,m^{-2}}$.

shown. The red dashed line is the average void fraction of the clean bed and the red dotted line is the average void fraction of a contaminated packed bed which is calculated using the measured powder hold-up of $60\,\mathrm{kg\,m^{-2}}$. Together with the data (pressure drop) presented in Fig. 7 the *Molerus* Eq. (2) is used to estimate the void fraction inside the packed for different vertical positions. These calculations are validated by comparing them to the total powder hold-up determined by the powder mass balance. The results are presented as red bars in Fig. 7 and indicate, that only the void fraction in the top fifth of the packed bed (between measuring points 1 and 3) is significantly lower than the void fraction of the clean packed bed. In addition to these calculated results Fig. 8 shows the packed bed in the PBTES test rig at three different states. In the left picture a clean packed bed is depicted. The center picture shows the top surface (where the gas-powder two phase flow enters the packed bed) of a packed bed with a powder hold-up of $30\,\mathrm{kg\,m^{-2}}$. The right picture is taken from the same angle after the top fifth of the packed bed is removed. As was already assumed when interpreting the data in Figs. 5–7, Fig. 8 shows that most of the powder hold-up in the packed bed is concentrated near the top surface of the packed bed. Furthermore the center and right photographs in Fig. 8 show an even radial distribution of the powder hold-up which indicates a uniform perfusion of the packed bed even with a significant amount of powder hold-up. After each experiment the contaminated storage material was removed layer-by-layer and the packed bed was checked for any areas with more powder accumulation than in others. After none of the experiments any irregularities in the uniformity of the powder accumulation could be detected. The detailed examination of the packed bed during and after each experiment suggests that there is no risk of random flow channel formation through the packed bed.

4.2. Influence of powder/fluid mass flux

The trend of the pressure drop for a charging period of 80 min is depicted in Fig. 9. This figure shows the relative pressure drop between the upper- and lowermost pressure measuring points $\Delta\hat{p}_{1-11}$ of the test rig for two powder mass fluxes and a fluid mass flux of $0.4\,\mathrm{kg\,m^{-2}\,s^{-1}}$. These results show that the pressure drop of a PBTES that is charged with a gas-powder two phase exhaust gas increases exponentially over

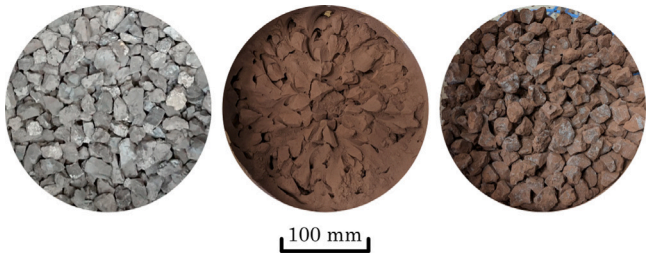

Fig. 8. Photograph of a clean packed bed (left) and a packed bed with a powder hold-up of $60\,\mathrm{kg\,m^{-2}}$: top view directly after charging (center), top view after charging and after removing the upper fifth of the packed bed (right).

time. After a charging period of 50 min with a powder mass flux of $17\,\mathrm{kg\,m^{-2}\,s^{-1}}$ an increase of the pressure drop by a factor of up to 4.5 is observed. A reduction of the powder mass flux also leads to a slower increase of the pressure drop, however, no saturation effects could be observed in any of the experiments. This means, that independent of the powder mass flux, powder will continue to accumulate over time which leads to a reduced exergy efficiency of the TES due to the increased pressure drop and eventually a clogging of the packed bed. Hence, frequent maintenance intervals at which the packed bed is cleaned or renewed are necessary. The frequency of maintenance can only be reduced by reducing the powder content of the fluid that passes through the packed bed. This could be realized by using a drop-out box that separates the coarse powder fractions from the HTF before it enters the PBTES.

In Fig. 10 the impact of the fluid mass flux on the trend of the relative pressure drop of the packed bed is shown. It can be seen that a reduction of the fluid mass flux leads to a much faster increase of the relative pressure drop with respect to the powder hold-up in the packed bed. Notice, that in both cases the powder content of the fluid is 0.042 kg powder per kg fluid and the abscissa in Fig. 10 represents the powder hold-up in the packed bed and not the charging time. As a higher fluid mass flux with the same powder content also means a higher powder mass flux, the difference with respect to the charging time would not be as pronounced, but still present. The reason for that is based on the elutriation velocity of the powder particles which is (among other factors) mainly determined by its size. The smaller the

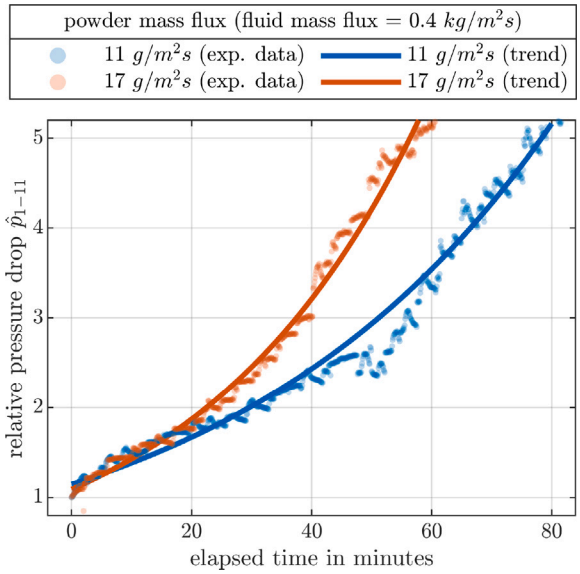

Fig. 9. Impact of the powder mass flux on the pressure drop of a packed bed that is operated with a gas-powder two phase flow.

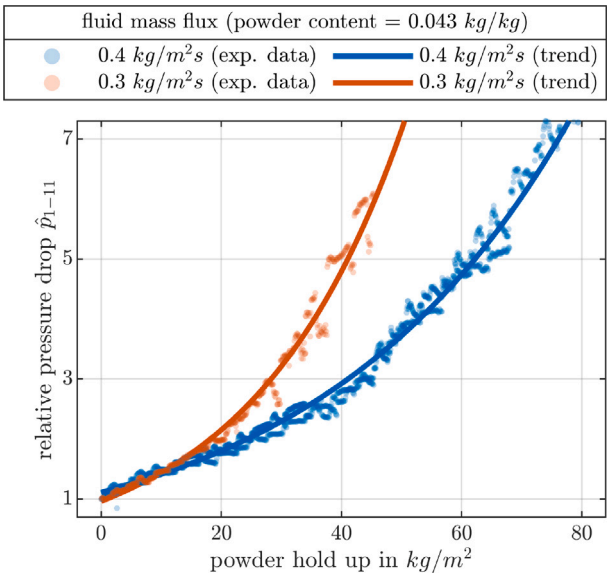

Fig. 10. Impact of the fluid mass flux on the pressure drop of a packed bed that is operated with a gas-powder two phase flow.

particle, the lower its elutriation velocity and vice versa. For the present use-case this means that all powder particles with an elutriation velocity higher than the velocity of the fluid passing through the packed bed will accumulate in the packed bed. Powder particles with an elutriation velocity that is lower than the fluid velocity remain in the fluid flow and pass through the packed bed. Nevertheless, the data in Fig. 10 allows to make some important statements about the preferred operation strategy of a PBTES that is charged with a gas-powder two phase flow. Fig. 10 shows that a powder hold-up of $40\,\mathrm{kg\,m^{-2}}$ increases the pressure drop of a PBTES that is charged with a fluid mass flux of 0.3 and $0.4\,\mathrm{kg\,m^{-2}\,s^{-1}}$ by a factor of 5 and 3 respectively. This observation combined with the fact that both experiments were conducted with HTF having the same powder content means that the higher the HTF mass flux, i.e. the thermal power rate, at which the PBTES is charged, the slower the decrease of the storage's exergy efficiency due to the increased pressure drop. For the operation of a PBTES that is charged with a gas-powder two phase flow this implies, that high charging power rates should be preferred to reduce the impact of powder hold-up on the pressure drop and hence the systems exergy efficiency.

4.3. Summary and discussion

The proposed integration of a PBTES for the waste heat recovery in the iron and steel industry is attractive because of its simplicity and its energetic and economic benefits. Excess heat from steel producing processes that is available as hot gas-powder two phase exhaust gas can be stored in a PBTES by directly using the exhaust gas as HTF. Due to the considerably uniform distribution of the powder hold-up in radial direction there is little risk of thermal performance degradation (storage capacity, thermal power rate) of the storage caused by random flow channel formation. As clean HTF that is used to discharge the PBTES is not contaminated by powder hold-up in the PBTES, heat recovered from the storage can be used in conventional waste heat boilers or for preheating purposes.

However, the results also show that there still is need for research and development work in order to make PBTES systems suitable for waste heat recovery in the iron and steel industry. The main challenge in this context is to find an operating/maintenance strategy to keep the pressure drop of HTF passing through the packed bed within appropriate bounds. It is important to keep the pressure drop of HTF passing through the packed bed as low as possible as the exergy efficiency of a PBTES is strongly influenced by the energy needed to pump HTF through the packed bed. Considering the results presented in this study strategies and technologies to reduction of the powder content of the HTF before it enters the PBTES and to reduce the amount of powder hold-up that accumulates in the PBTES are required. The powder content of the HTF can be reduce with existing technologies like gravity separators (drop-out boxes). An interesting approach to reduce the powder hold-up in the packed bed is to switch the flow direction for the charging and discharging process of the PBTES (charging from bottom and discharging from top) and to utilize periodic knocking/trembling mechanisms to clean the packed bed from the accumulated powder hold-up. As the powder hold-up in the PBTES concentrates near the surface at which the HTF enters the packed bed, which, for switched flow directions would be the bottom surface of the bed, the removal of the powder hold-up takes place by gravitation. The limitations and possible challenges this approach could entail include a reduced exergy efficiency of the storage due to thermocline degradation especially during long standby periods. For details considering these effects the authors refer to their previous work [18].

5. Conclusion

The present study examined the suitability of packed bed thermal energy storage systems for the waste heat recovery in the iron and steel industry. Besides extreme temperatures and the highly fluctuating and unpredictable availability of excess heat, the main difficulty of waste heat recovery in industrial processes is the high amount of powder that is transported by the hot exhaust gases. Therefore the focus of this study was the investigation of the behavior/characteristics of a packed bed thermal energy storage that is operated with a gas-powder two phase heat transfer fluid.

A lab-scale test rig of a packed bed thermal energy storage was used to quantify the pressure drop and powder hold-up that have to be expected when a packed bed thermal energy storage is operated with a gas-powder two phase heat transfer fluid.

The investigations revealed that, for the given materials and operational parameters, 98 % of the powder that enters the test rig when it is charged with a gas-powder two phase fluid accumulates in the packed bed. Only the finest fractions (2 %) of the powder remain in the fluid flow passing through the packed bed. Furthermore, reversing the flow direction of the heat transfer fluid and discharging the test rig with a clean single phase fluid does not lead to a reduction of the powder hold-up inside the packed bed. Hence, clean fluid that is used to discharge the test rig is not contaminated with the powder hold-up in the packed bed. Additionally an uneven distribution of the powder hold-up along the fluid flow direction was observed by examining the packed bed after the experiments. These observations are consistent with the pressure drop measurements during the experiments. A large proportion of the powder hold-up is concentrated near the surface at which the fluid flow enters the packed bed. The distribution of powder hold-up in radial direction of the test rig was observed to be uniform and no random flow channel formation could be detected.

Overall, the integration of a packed bed thermal energy storage as waste heat recovery system in the iron and steel industry was found to be suitable and is definitely worth further investigation. Especially the evaluation and development of suitable strategies for the removal of powder hold-up from the storage material should be the main focus in future research projects.

CRediT authorship contribution statement

Paul Schwarzmayr: Conceptualization, Methodology, Validation, Formal analysis, Investigation, Data curation, Writing – original draft, Visualization. **Felix Birkelbach:** Conceptualization, Methodology, Formal analysis, Writing – review & editing. **Heimo Walter:** Conceptualization, Methodology, Formal analysis, Writing – review & editing,

Visualization, Supervision. **Florian Javernik:** Conceptualization, Resources, Writing – review & editing, Project administration, Funding acquisition. **Michael Schwaiger:** Conceptualization, Resources, Writing – review & editing, Project administration, Funding acquisition. **René Hofmann:** Conceptualization, Validation, Writing – review & editing, Supervision, Funding acquisition.

Declaration of competing interest

The authors declare that they have no known competing financial interests or personal relationships that could have appeared to influence the work reported in this paper.

Data availability

Data will be made available on request.

Acknowledgments

The authors acknowledge funding support of this work through the research project *5DIndustrialTwin* as part of the Austrian Climate and Energy Fund's initiative Energieforschung (e!MISSION) 6th call (FFG project number 881140). Furthermore, the authors acknowledge TU Wien Bibliothek, Austria for financial support through its Open Access Funding programme.

References

[1] L. Miró, J. Gasia, L.F. Cabeza, Thermal energy storage (TES) for industrial waste heat (IWH) recovery: A review, Appl. Energy 179 (2016) 284–301, http://dx.doi.org/10.1016/j.apenergy.2016.06.147.

[2] G. Manente, Y. Ding, A. Sciacovelli, A structured procedure for the selection of thermal energy storage options for utilization and conversion of industrial waste heat, J. Energy Storage 51 (2022) 104411, http://dx.doi.org/10.1016/j.est.2022.104411.

[3] L. Geissbühler, A. Mathur, A. Mularczyk, A. Haselbacher, An assessment of thermocline-control methods for packed-bed thermal-energy storage in CSP plants, Part 1: Method descriptions, Sol. Energy 178 (2019) 341–350, http://dx.doi.org/10.1016/j.solener.2018.12.015.

[4] L. Geissbühler, A. Mathur, A. Mularczyk, A. Haselbacher, An assessment of thermocline-control methods for packed-bed thermal-energy storage in CSP plants, Part 2: Assessment strategy and results, Sol. Energy 178 (2019) 351–364, http://dx.doi.org/10.1016/j.solener.2018.12.016.

[5] I. Ortega-Fernández, J. Rodríguez-Aseguinolaza, Thermal energy storage for waste heat recovery in the steelworks: The case study of the REslag project, Appl. Energy 237 (2019) 708–719, http://dx.doi.org/10.1016/j.apenergy.2019.01.007.

[6] H. Slimani, Y. Filali Baba, H. Ait Ousaleh, A. Elharrak, F. El Hamdani, H. Bouzekri, A. Al Mers, A. Faik, Horizontal thermal energy storage system for Moroccan steel and iron industry waste heat recovery: Numerical and economic study, J. Clean. Prod. 393 (2023) 136176, http://dx.doi.org/10.1016/j.jclepro.2023.136176.

[7] G.S. Gupta, S. Lakshminarasimha, M. Shrenik, Quantitative measurement of powder holdups in the packed beds, Trans. Indian Inst. Met. 75 (2) (2022) 381–395, http://dx.doi.org/10.1007/s12666-021-02431-2.

[8] H. Zhou, X. Tian, M. Kou, S. Wu, Y. Shen, Numerical study of fine particles behaviors in a packed bed with lateral injection using CFD-DEM, Powder Technol. 392 (2021) 317–324, http://dx.doi.org/10.1016/j.powtec.2021.07.019.

[9] X.F. Dong, S.J. Zhang, D. Pinson, A.B. Yu, P. Zulli, Gas–powder flow and powder accumulation in a packed bed: II: Numerical study, Powder Technol. 149 (1) (2004) 10–22, http://dx.doi.org/10.1016/j.powtec.2004.09.039.

[10] X.F. Dong, D. Pinson, S.J. Zhang, A.B. Yu, P. Zulli, Gas–powder flow and powder accumulation in a packed bed: I. Experimental study, Powder Technol. 149 (1) (2004) 1–9, http://dx.doi.org/10.1016/j.powtec.2004.09.040.

[11] H. Takahashi, H. Kawai, T. Kondo, M. Sugawara, Permeation and blockage of fine particles transported by updraft through a packed bed, ISIJ Int. 51 (10) (2011) 1608–1616, http://dx.doi.org/10.2355/isijinternational.51.1608.

[12] S. Kiochiro, S. Masakata, I. Shin-ichi, T. Reijiro, Y. Jun-ichiro, Pressure loss and hold-up powders for gas-powder two phase flow in packed beds, ISIJ Int. 31 (5) (1991) 434–439, http://dx.doi.org/10.2355/isijinternational.31.434.

[13] Mastersizer 3000 - Particle Size Analyzer | Malvern Panalytical.

[14] Aero S - Dry Powder Dispersion Unit | Malvern Panalytical.

[15] W. Kast, H. Nirschl, W. Kast, H. Nirschl, W. Kast, H. Nirschl, E.S. Gaddis, E.S. Gaddis, K.-E. Wirth, J. Stichlmair, L1 Einphasige Strömungen, in: VDI-WäRmeatlas, in: VDI-Buch, Springer, Berlin, Heidelberg, 2013, pp. 1221–1284, http://dx.doi.org/10.1007/978-3-642-19981-3_74.

[16] S. Ergun, Fluid flow through packed columns, Chem. Eng. Prog. 48 (2) (1952) 89–94.

[17] O. Molerus, Kohärente Darstellung des Druckverlustverhaltens von Festbetten und des Ausdehnungsverhaltens homogener (Flüssigkeits-/Feststoff-) Wirbelschichten, in: O. Molerus (Ed.), Fluid-Feststoff-Strömungen: Strömungsverhalten Feststoffbeladener Fluide Und KohäSiver Schüttgüter, Springer, Berlin, Heidelberg, 1982, pp. 8–38, http://dx.doi.org/10.1007/978-3-642-50215-6_2.

[18] P. Schwarzmayr, F. Birkelbach, H. Walter, R. Hofmann, Standby efficiency and thermocline degradation of a packed bed thermal energy storage: An experimental study, Appl. Energy 337 (2023) 120917, http://dx.doi.org/10.1016/j.apenergy.2023.120917.